ISBN: 978-3-95450-208-0 doi:10.18429/JACoW-IPAC2019-MOPTS024

RECONSTRUCTION OF THE LONGITUDINAL PHASE PORTRAIT FOR THE SC CW HEAVY ION HELIAC AT GSI

S. Lauber*[1,2,4], K. Aulenbacher [1,2,4], W. Barth[1,2], C. Burandt[1,2], F. Dziuba[1,2,4], P. Forck[2], V. Gettmann[1,2], M. Heilmann[2], T. Kürzeder[1,2], J. List[1,2,4], M. Miski-Oglu[2], H. Podlech[3], A. Rubin[2], M. Schwarz[3], T. Sieber[2], S. Yaramyshev[2]
[1] Helmholtz Institute Mainz, Mainz, Germany
[2]GSI Helmholtzzentrum für Schwerionenforschung, Darmstadt, Germany
[3]Goethe-University, Frankfurt, Germany
[4]Johannes Gutenberg-University, Mainz, Germany

Abstract

At the GSI Helmholtzzentrum für Schwerionenforschung (GSI) in Darmstadt, Germany, the HElmholtz LInear ACcelerator (HELIAC) is currently under construction. The HELIAC comprises superconducting multigap Crossbar H-mode (SC CH) cavities. The input beam is delivered by an already existing High Charge Injector (HLI). For the further development of the accelerator a detailed knowledge of the input beam parameters to the SC section is necessary. A method for beam reconstruction is incorporated, which provides for longitudinal beam characteristics using measurements with a beam shape monitor and a particle simulation code. This finalizes the investigations on 6D beam parameters, following previous measurements in transversal phase space. The reconstruction of the longitudinal phase portrait is presented.

INTRODUCTION

The research for new Super Heavy Elements (SHE) is driven by fusion-evaporation reactions of medium to heavy ions. Coping with extremely small cross-sections a long beam time at high luminosity is crucial for the experiments [1, 2]. As the GSI Universal Linear Accelerator (UNILAC) [3–7] is going to be upgraded in order to deliver a high intensity beam to the Facility for Antiproton and Ion Research (FAIR) [6, 7] with a short pulse rate, which is opposing to the SHE requirements. Therefore, a dedicated continuous wave (CW) heavy ion linear accelerator (LINAC) is proposed at GSI and Helmholtz Institute Mainz (HIM) [8, 9] under key support of Goethe University Frankfurt (IAP) [10, 11] and in collaboration with Moscow Engineering Physics Institute (MEPhI) and Moscow Institute for Theoretical and Experimental Physics (KI-ITEP) [12, 13]. A CW LINAC is a essential part of different modern accelerator facilities, as for high energy accelerators for the Spallation Neutron Source (SNS) [14] or medium energy applications in isotope generation, material science and boron-neutron capture therapy [15]. Technological progress in superconducting radio frequency (SRF) technologies [16] through advances in SC CW LINAC development is therefore a strong contribution to the whole cavity accelerator development.

* s.lauber@gsi.de

Helmholtz Linear Accelerator

The HELIAC [17] comprises an injector LINAC and a superconducting main LINAC section. A radio frequency quadrupole (RFQ) and an interdigital H-Mode cavity (IH) together with two rebuncher cavities are going to deliver a 1.4 MeV/u heavy ion beam to the SC section. The SC section is composed of four cryomodules with compact SC CH cavities [11]. The main features of this accelerator are a variable output energy (see Table 1) and the capability to provide for continuous wave operation, while keeping the momentum spread low. With these design objectives, the

Table 1: HELIAC Design Specifications [17]

	Value
Mass/Charge	< 6
Frequency	216.816 MHz
Maximum beam current	1 mA
Injection energy	1.4 MeV/u
Variable output energy	3.5 MeV/u to 7.3 MeV/u
Output energy spread	±3 keV/u

HELIAC lines up with other ambitious LINAC projects at GSI, namely the FAIR proton LINAC [18], the UNILAC proton beam delivery [19–21], the linear heavy ion decelerator HITRAP (Heavy Ion TRAP) [22] and the LIGHT (Laser Ion Generation, Handling and Transport) facility for laser acceleration of protons and heavy ions [23].

Demonstrator Environment

For the measurement campaigns in 2017 and 2018, a demonstrator environment has been set up in order to validate the novel CH design [24, 25]. The existing HLI [26] delivers different heavy ion beams to the demonstrator cavity. As result of the KONUS beam dynamics [27] used for the HLI-IH cavity, a non-linear transformation of the longitudinal bunch shape is envisaged. This is caused by using different RF phases in each acceleration gap instead of applying −30 degree constantly. Two rebunchers, two quadrupole duplets and a quadrupole triplet are available to match the beam to the demonstrator; three beam steerers are operated to align the beam (see Fig. 1). Phase probe sensors are used to determine the beam energy with Time Of Flight

ISBN: 978-3-95450-208-0 doi:10.18429/JACoW-IPAC2019-MOPTS024

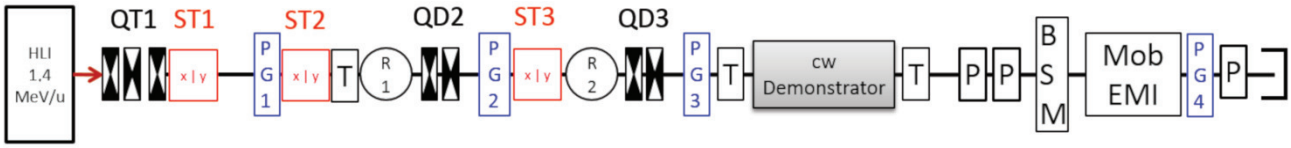

Figure 1: Beam line 2018. QT: Quadrupole Triplet, QD: Quadrupole Duplet, R: Rebuncher, X|Y: Beam Steerer, G: SEM-Grid, T: Beam Current Transformer, P: Phase Probe, BSM: Bunch Shape Monitor, EMI=Emittance Meter. [17]

(TOF) measurements. Secondary Electron EMission grids (SEM-Grid) provide for the beam profile and position. A Feschenko-Monitor [28] was used for investigations for the longitudinal bunch shape [29].

Principle of Tomographic Reconstruction

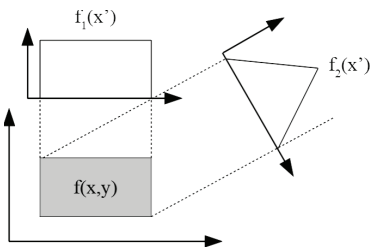

Figure 2: Example of reconstruction setup for a linear transformation between image and histogram. The observed histograms $f_i(x')$ constrain the shape of the reconstructed object.

Aim of the reconstruction is to infer the distribution $f(x, y)$ by a set of projections $f_i(x')$. The tomographic reconstruction method is applied in medical diagnostics where it is used for body imaging. A wide range of reconstruction algorithms already exist for clinical purpose, but are mostly formulated using linear mappings between $f(x, y)$ and $f_i(x')$ (see Fig. 2), or explicitly use rotation transformations. For accelerator applications, it is generally not possible to rotate the beam. Optical elements in the beam line are used to alter the bunch shape, which in most cases is characterized by a linear transformation. In this case, it is possible to preprocess the data into a sinogram and use this as input for common reconstruction algorithms. But in some cases, the bunch transfer is not linear, therefore it is not useful to use sinograms. Suitable algorithms have to be adapted to this scenarios. The Algebraic Reconstruction Technique (ART) [30] and the Maximum Entropy Tomography Reconstruction (MENT) [31] have been used for longitudinal phase space reconstruction [31, 32]. For the HELIAC, a different approach has been investigated. Rather than using ART or MENT, a Non Negative Least Squares (NNLS) [33] solver is used to reconstruct the longitudinal phase plane.

METHODS

For the reconstruction, different projections must be obtained. Therefore, the two rebunchers were used to provide diverse bunch shapes at the Bunch Shape Monitor (BSM).

Bunch Shape Monitor

For the series of measurements, which were used as input for the reconstruction algorithm, a Feschenko Monitor was mounted behind the demonstrator. The device provides for measurements of the longitudinal bunch shape of heavy ions and offers a high signal to noise ratio and a phase resolution of up to 1 deg with respect to 108.408 MHz. A detailed description of the Feschenko Monitor is given in [28].

Reconstruction

For the reconstruction, the relation from the input coordinates at the start of the beam line i.e. at the exit of the HLI to the coordinates at the Feschenko Monitor must be known. The beamline could be described by using the particle tracking code DYNAMION [34], which allows to monitor individual particles along their trajectory. Disposing a grid as input distribution and tracking it through the beamline, the mapping from HLI to BSM $\vec{f}_i(\vec{x}_{\text{in}})$ could be described for each buncher setting i, as well as the the projection to the longitudinal spatial axis $A_i(\phi, \vec{X}_{\text{in}})$ for a set of input coordinates $\vec{X}_{\text{in}}$. For a given particle output phase ϕ, a set of input coordinates $\vec{x}_{\text{in},i}$ exists: $\vec{x}_{\text{in},i}(\phi)$ is ambiguous. In order to determine the boundaries, which are used for NNLS reconstruction, the back tracking function $\vec{x}_{\text{in},i}(\phi)$ can be used to select the area to reconstruct for. All phases ϕ where the signal is zero are selected and tracked back for each histogram. Two areas can be distinguished: areas with signal and areas without signal. By summing up these areas of every histogram, an image can be produced, describing the amount of histograms holding signal/no signal: $N_i(\vec{x}_{\text{in}}) = |\{\phi_i(\vec{x}_{\text{in}})|A(\phi_i(\vec{x}_{in})) \neq 0\}|$.

Furthermore, the mapping $A_i(\phi, \vec{X}_{\text{in}})$ can be expressed in terms of a matrix multiplication $\vec{A}_i = B_i \cdot \vec{X}$ for discrete values $\vec{f}_i(\phi, p)$, which are assembled into X. With this discretization, also nonlinear mappings can be expressed in terms of B_i, which comes in handy when solving for the input distribution $\vec{X}$ with given measurements $\vec{A}_i$. Therefore, all mappings and all measurements can be stacked up into one equation $\vec{A} = B \cdot \vec{X}$. Also, a negative particle count for the input distribution is not considered. Therefore the task can be expressed as Non Negative Least Squares problem:

$$\text{argmin}_{\vec{X}} ||B\vec{X} - \vec{A}||_2 \text{ subject to } \vec{X} \geq 0 \quad (1)$$

ISBN: 978-3-95450-208-0 doi:10.18429/JACoW-IPAC2019-MOPTS024

RESULTS

Measurements

The matching line (excluding the rebunchers) was optimized for minimal beam loss for a wide range of rebuncher settings. A set of 100 BSM-measurements has been conducted for an Ar^{9+} beam from the HLI. Combinations of different rebuncher voltages ($R1$,$R2$) were applied, providing for a transition from defocusing to overfocusing. Exemplary measurements are presented in Fig. 3.

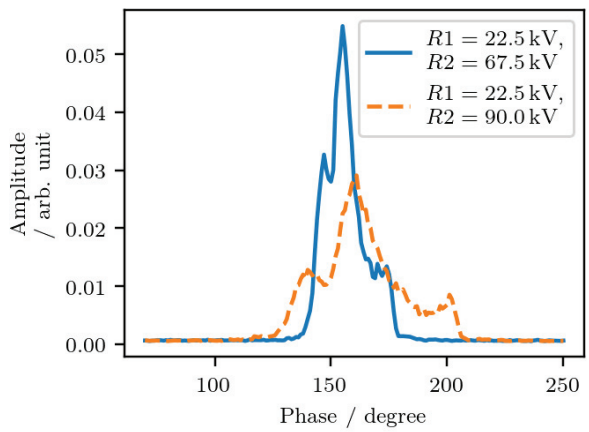

Figure 3: Measured bunch shape samples for different rebuncher settings measured with the BSM.

As expected, the beam shape is not elliptic due to the KONUS beam dynamics of the HLI-IH-DTL. This makes the use of an advanced reconstruction technique necessary, which considers a non elliptic shape. Conservative preprocessing was applied to the measurement data. 6 % of the amplitudes were cut to remove unwanted background. The histograms were recentered to their center of mass. In good accordance to the measurements the transmission was assumed to be 100 %.

Reconstruction

As described in the previous section, the back projection of the histograms can be used to determine the area of the bunch in the longitudinal phase space. These limits can be used as constraints of the NNLS solver. Due to the back projection properties, a signal of 0 % can not be achieved by overlapping projections from different "directions". The RMS-emittance of the yellow (100 %) area could be evaluated for $\epsilon_{\mathrm{RMS}} = 0.47\,\mathrm{keV/u\,ns}$. This result is in good agreement with the former HLI simulations, yielding an RMS emittance of 0.347 keV/u ns. The reconstructed emittance could occur slightly increased, because our shape reconstruction does not distinguish between low and high signal strengths. Inside the limits shown in Fig. 4, the NNLS solver was applied to reconstruct the predefined area on base of the measurements. A complicated shape is revealed (see Fig. 5). The full emittance is $\epsilon_{\mathrm{RMS}} = 0.7\,\mathrm{keV/u\,ns}$. A remarkably small spot with high intensity is visible. Verification measurements are scheduled to compare the BSM measurements behind the HLI to the reconstructed bunch shape.

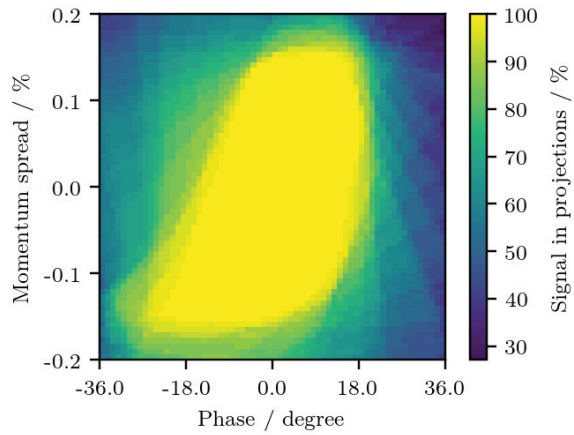

Figure 4: By back projecting the histograms to the input plane, areas can be marked where signal is absent and vice versa.

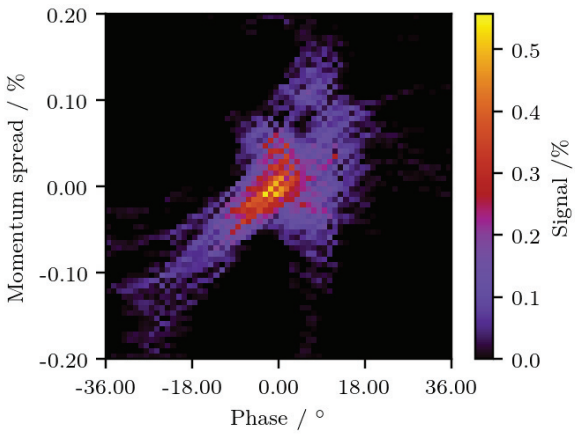

Figure 5: Reconstructed phase space with the NNLS solver. The head of the bunch is displayed on the right side, the tail on the left.

CONCLUSION

A set of measurements has been carried out, which allows to reconstruct the bunch shape with various solvers. The boundaries for the phase space reconstruction have been found. A reliable algorithm is used to obtain the density distribution inside the assumed limits. With the newly developed method it is possible to determine how the parameters of the HLI affect the longitudinal output beam shape. A second measurement campaign is scheduled, where the BSM is mounted at the HLI exit, which allows to compare the reconstructed beam shape projection with a direct measurement.

ISBN: 978-3-95450-208-0 doi:10.18429/JACoW-IPAC2019-MOPTS024

REFERENCES

[1] M. Block *et al.*, "Direct mass measurements above uranium bridge the gap to the island of stability", *Nature*, vol. 463, pp. 785–788, Feb. 2010.

[2] J. Khuyagbaatar *et al.*, "48Ca + 249Bk Fusion Reaction Leading to Element Z=117: Long-Lived α-Decaying 270Db and Discovery of 266Lr", *Phys. Rev. Lett.*, vol. 112, no. 17, p. 172501, May 2014.

[3] W. Barth *et al.*, "U28+ intensity record applying a H2 gas stripper cell", *Phys. Rev. ST Accel. Beams*, vol 18, p. 040101, Apr. 2015.

[4] A. Adonin *et al.*, "Beam brilliance investigation of high current ion beams at GSI heavy ion accelerator facility", *Rev. Sci. Instrum.*, vol. 85, p. 02A727, Apr. 2014.

[5] S. Yaramyshev *et al.*, "Virtual charge state separator as an advanced tool coupling measurements and simulations", *Phys. Rev. ST Accel. Beams*, vol. 18, p. 050103, Sept. 2015.

[6] W. Barth *et al.*, "High brilliance uranium beams for the GSI FAIR", *Phys. Rev. ST Accel. Beams*, vol. 20, p. 050101, May 2017.

[7] W. Barth *et al.*, "Upgrade program of the high current heavy ion UNILAC as an injector for FAIR", *Nucl. Instr. Meth. Phys. Res. Sect. A*, vol. 577, no. 1-2, pp. 211–214, Jul. 2007.

[8] W. Barth *et al.*, "Superconducting CH-Cavity Heavy Ion Beam Testing at GSI", *J. Phys. Conf. Ser.*, vol. 1067, no. 5, p. 052007, Sept. 2018.

[9] F. Dziuba *et al.*, First Cold Tests of the Superconducting cw Demonstrator at GSI, in *Proc. RuPAC'16*, St. Petersburg, Russia, Nov. 2016, p. 83-85.

[10] H. Podlech *et al.*, "Superconducting CH structure", *Phys. Rev. ST Accel. Beams*, vol. 10, no. 8, p. 080101, Aug. 2007.

[11] M. Schwarz *et al.*, "Beam Dynamics Simulations for the New Superconducting CW Heavy Ion LINAC at GSI", *J. Phys.: Conf. Ser.*, vol. 1067, 052006, Oct. 2018.

[12] M. Gusarova *et al.*, "Design of the two-gap superconducting re-buncher", *J. Phys.: Conf. Ser.*, vol. 1067, p. 082005, Oct. 2018.

[13] K. Taletskiy *et al.*, "Comparative study of low beta multi-gap superconducting bunchers", *J. Phys.: Conf. Ser.*, vol. 1067, p. 082006, Oct. 2018.

[14] S.M. Polozov and A.D. Fertman, "High-energy proton beam accelerators for subcritical nuclear reactors", *At. Energ.*, vol. 113, no. 3, pp. 192–200, Jan. 2013.

[15] Zhi-Jun Wang *et al.*, "Beam commissioning for a superconducting proton linac", *Phys. Rev. Accel. Beams*, vol 19, p. 120101, Dec. 2016.

[16] R. Laxdal *et al.*, "Recent progress in the superconducting RF Program at TRIUMF/ISAC", *Physica C: Superconductivity* vol. 441, no. 1-2, pp. 13, Jul. 2006.

[17] W. Barth *et al.*, "First heavy ion beam tests with a superconducting multigap CH cavity", *Phy. Rev. Accel. Beams*, vol. 21, no. 2, p. 020102, Feb. 2018.

[18] U. Ratzinger *et al.*, "The 70 MeV p-injector design for FAIR", *AIP Conf. Proc.*, Vol. 773, pp 249-253, 2005.

[19] W. Barth *et al.*, "Heavy ion linac as a high current proton beam injector", *Phys. Rev. ST Accel. Beams*, vol. 18,p. 050102, Sep. 2015.

[20] A. Adonin *et al.*, "Production of high current proton beams using complex H-rich molecules at GSI", *Rev. Sci. Instrum.*, vol. 87, 02B709, 2016.

[21] P. Forck, "Minimal invasive beam profile monitors for high intense hadron beams", in *Proc. IPAC'10*, Kyoto, Japan, May 2010, pp. 1261-1265.

[22] F. Herfurth *et al.*, "The HITRAP facility for slow highly charged ions", *Physica Scripta* vol. 2015, no. T166, 014065, Nov. 2015.

[23] S. Busold *et al.*, "Shaping laser accelerated ions for future applications - The LIGHT collaboration", *Nucl. Instrum. Meth. Phys. Res. Sect. A*, vol. 740, pp. 94-98, Mar. 2014.

[24] S. Yaramyshev *et al.*, "Advanced Approach for Beam Matching along the Multi-Cavity SC CW Linac at GSI", *J. Phys. Conf. Ser.*, vol. 1067, p. 052005, Sep. 2018.

[25] S. Minaev *et al.*, "Superconducting, energy variable heavy ion linac with constant β, multicell cavities of CH-type", *Phys. Rev. ST Accel. Beams*, vol. 12, p. 120101, Dec. 2009.

[26] P. Gerhard *et al.*, "Commissioning of a new cw radio frequency quadrupole at GSI", in *Proc. IPAC'10*, Kyoto, Japan, May 2010, pp. 741–743.

[27] R. Tiede *et al.*, "LORASR Code Development", Proc. 10th Europ. Particle Accelerator Conf. (EPAC'06), Edinburgh, Scotland, 2006, paper WEPCH118, pp. 2194–2196.

[28] A. V. Feschenko, "Methods and Instrumentation for Bunch Shape Measurements" in *Proc. PAC2001* vol. 1, Chicago, IL, USA , Jun. 2001, pp. 517-521.

[29] T. Sieber *et al.*, "Bunch Shape Measurements at the GSI cw-Linac Prototype", in Proc. IPAC'18, Vancouver, Canada, 2018, pp. 2091-2094.

[30] R. Gordon, R. Bender, and G. T. Herman, "Algebraic Reconstruction Techniques (ART) for three-dimensional electron microscopy and X-ray photography", *Journal of Theoretical Biology*, vol. 29, no. 3, pp. 471-476, Dec. 1970.

[31] K. M. Hock *et al.*, "Beam tomography research at Daresbury Laboratory", *Nucl. Instr. Meth. Phys. Res. Sect. A*, vol. 753, no. 1, pp. 38-55, Jul. 2014.

[32] D. Malyutin *et al.*, "Longitudinal phase space tomography using a booster cavity at PITZ", *Nucl. Instr. Meth. Phys. Res. Sect. A*, vol. 871, no. 1, Nov. 2017, pp. 105-112.

[33] C. L. Lawson and R. J. Hanson, *Solving Least Squares Problems*. Philadelphia, PA, USA: Society for Industrial and Applied Mathematics, 1987.

[34] S. Yaramyshev *et al.*, "Development of the versatile multi-particle code DYNAMION", *Nucl. Instrum. Meth. Phys. Res. Sect. A*, vol. 558, no. 1, p. 90-95, Mar. 2006.